

Higher Nucleon Resonances in Exclusive $(\gamma, \pi N)$ Reactions on Nuclei

Frank X. Lee ¹ *, Cornelius Bennhold ², Sabit S. Kamalov ³ †, Louis E. Wright ⁴

¹ *Nuclear Physics Laboratory, Department of Physics, University of Colorado,
Boulder, CO 80309*

² *Center for Nuclear Studies, Department of Physics, The George Washington University,
Washington, DC 20052*

³ *Institut für Kernphysik, Johannes Gutenberg-Universität, D-55099 Mainz, Germany*

⁴ *Institute of Nuclear and Particle Physics, Department of Physics and Astronomy,
Ohio University, Athens, OH 45701*

Abstract

We report calculations for exclusive pion photoproduction on nuclei beyond the first resonance region in the distorted wave impulse approximation. The elementary operator contains contributions from the resonances $P_{33}(1232)$, $P_{11}(1440)$, $D_{13}(1520)$, $D_{33}(1740)$, $S_{11}(1535)$, $S_{11}(1650)$, and $F_{15}(1680)$, in addition to the usual Born plus vector meson contributions. It gives a good description of single pion photoproduction data up to about 1.1 GeV. Final state interactions are incorporated via optical potentials and are found to be substantial in the coincidence cross sections, but insensitive to the photon

*Address after 24 August 1998: Department of Physics, The George Washington University, Washington, DC 20052

†On leave from Laboratory of Theoretical Physics, JINR Dubna, SU-101000 Moscow, Russia.

asymmetry. Clear signatures of possible medium modifications of the D_{13} and F_{15} resonances are predicted.

PACS numbers: 25.20.Lj, 13.60.Le, 14.20.Gk

I. INTRODUCTION

Meson photoproduction has been a valuable source of information on the structure of hadrons and nuclei. With the advent of the new generation of high-intensity continuous-wave electron accelerators, as represented by the Jefferson Lab, the field reaches a new level of promise. The new facilities allow exclusive measurements with unprecedented precision under a variety of kinematical conditions, thus making it possible to study higher excited states of hadrons in greater detail.

The elementary single pion photoproduction (with four possible channels),

$$\gamma + N \rightarrow \pi + N, \tag{1}$$

has been the subject of extensive study both theoretically and experimentally over the last two decades. In the energy range from threshold through the delta resonance region, a progressive series of models based on the effective Lagrangian approach at tree level have been developed [1,2] which have generally provided an adequate description of available cross section data. More complete descriptions include final state rescattering by iterating the full scattering equation [3–7], thus incorporating unitarity dynamically. Attempts to extend the tree-level approach beyond the delta resonance region have been made in recent years in Ref. [8] and Ref. [9] for energies up to around $E_\gamma=1$ GeV. At even higher energies ($E_\gamma \geq 4$ GeV), a model for pion and kaon photo- and electroproduction by Guidal *et. al.* [10] has been developed based on Regge theory. A fairly complete compilation of the data below 2 GeV has been maintained by the VPI group [12] and by the KEK group [13].

Using a newly developed operator, we carry out nuclear calculations in this work for the exclusive reactions, $A(\gamma, \pi N)A - 1$, beyond the first resonance region in a distorted wave impulse approximation (DWIA) framework. Pion photoproduction on a nucleus provides a different environment in which the reaction can take place. Issues arise such as the nuclear reaction mechanism, the interaction of the resonances with the medium, and the final state interactions. Our focus is on the puzzle of the ‘damped resonances’ in the second and

third resonance regions as seen in inclusive photoabsorption cross section data on various nuclei [14]. The data show an unexpected damping behavior of the higher resonances when compared with the same process on the proton and the deuteron. Clearly, in order to isolate the mechanism for this mysterious phenomenon the individual exclusive channels need to be investigated.

Quasifree pion photoproduction allows for the study of the production process in the nuclear medium as well as final state interaction effects without being obscured by the details of the nuclear transition. This is due mainly to the quasifree nature of the reaction which permits the kinematic flexibility to have small momentum transfers. Conceptually, the initial nucleus is a target holder which presents a bound nucleon to the incoming photon beam. The basic reaction $N(\gamma, \pi N)$ takes place in the nuclear medium producing a continuum pion and nucleon which interact with the residual nucleus as they exit the target. The key ingredients in such a description are: a) the single-particle wave function of the initial nucleon and spectroscopic factor, usually taken from electron scattering, b) the elementary pion photoproduction amplitudes, obtained from measuring the free processes, c) the nucleon-nucleus final state interaction, taken from elastic scattering, and finally, d) the pion-nucleus final state interaction, also taken from elastic scattering.

The ability of the reaction in studying these issues has been demonstrated in our previous works on pion photoproduction [15] and electroproduction [16] from nuclei in the delta resonance region. It was found that the DWIA model gave an adequate description of these reactions when compared to data without including any damping mechanisms for the delta resonance. The model was also applied to eta photoproduction from nuclei [17], and to kaon photoproduction from nuclei [18] to investigate the possibility of using the reaction to extract information about hyperon-nucleus interactions.

Section II outlines the key elements in the DWIA model. Section III discusses some dynamical features of the basic production operator and reports our results on nuclei under quasifree kinematics. Section IV contains the concluding remarks.

II. THE DWIA MODEL

Consider the process in the laboratory frame where the target is at rest. The coordinate system is defined such that the z-axis is along the photon direction \mathbf{p}_γ , and the y-axis is along $\mathbf{p}_\gamma \times \mathbf{p}_\pi$ with the azimuthal angle of the pion chosen as $\phi_\pi = 0$. The kinematics of the reaction are determined by

$$\mathbf{p}_\gamma = \mathbf{p}_\pi + \mathbf{p}_N + \mathbf{p}_m, \quad (2)$$

$$E_\gamma + M_i = E_\pi + E_N + M_f + T_m. \quad (3)$$

Here \mathbf{p}_m is the missing momentum in the reaction and $T_m = \frac{p_m^2}{2M_f}$ is the recoil kinetic energy. The excitation energy of the residual nucleus is included in M_f . The missing energy E_m in the reaction is defined by $E_m = M_f - M_i + m_N = E_\gamma - E_\pi - E_N - T_m + m_N$ where m_N is the mass of the nucleon. For real photons, $|\mathbf{p}_\gamma| = E_\gamma$. In the impulse approximation, the reaction is assumed to take place on a single bound nucleon whose momentum and energy are given by $\mathbf{p}_i = -\mathbf{p}_m$ and $E_i = E_\pi + E_N - E_\gamma$. The struck nucleon is in general off its mass shell.

The reaction is *quasifree*, meaning that the magnitude of \mathbf{p}_m has a wide range, including zero. Since the reaction amplitude is proportional to the Fourier transform of the bound state single particle wavefunction, it falls off quickly as the momentum transfer increases. Thus we will restrict ourselves in the low p_m region (< 400 MeV/c) where the nuclear recoil effects (T_m) can be safely neglected for nuclei of $A > 6$.

The differential cross section can be written as

$$\frac{d^3\sigma}{dE_\pi d\Omega_\pi d\Omega_N} = \frac{C}{2(2J_i + 1)} \sum_{\alpha, \lambda, m_s} \frac{S_\alpha}{2(2j + 1)} |T(\alpha, \lambda, m_s)|^2. \quad (4)$$

The kinematical factor is given by

$$C = \frac{M_f m_N |\mathbf{p}_\pi| |\mathbf{p}_N|}{4(2\pi)^5 |E_N + M_f + T_m - E_N \mathbf{p}_N \cdot (\mathbf{p}_\gamma - \mathbf{p}_m) / p_N^2|}. \quad (5)$$

The single particle matrix element is given by

$$T(\alpha, \lambda, m_s) = \int d^3r \Psi_{m_s}^{(+)}(\mathbf{r}, -\mathbf{p}_N) \phi_{\pi}^{(+)}(\mathbf{r}, -\mathbf{p}_{\pi}) t_{\gamma\pi}(\lambda, \mathbf{p}_{\gamma}, \mathbf{p}_i, \mathbf{p}_{\pi}, \mathbf{p}_N) \Psi_{\alpha}(\mathbf{r}) e^{i\mathbf{p}_{\gamma}\cdot\mathbf{r}}. \quad (6)$$

In the above equations, J_i is the target spin, $\alpha = \{nljm\}$ represents the single particle states, S_{α} is called the spectroscopic factor, λ is the photon polarization, m_s is the spin projection of the outgoing nucleon, $\Psi_{m_s}^{(+)}$ and $\phi_{\pi}^{(+)}$ are the distorted wavefunctions with outgoing boundary conditions, Ψ_{α} is the bound nucleon wavefunction, and $t_{\gamma\pi}$ is the pion photoproduction operator.

In addition to cross sections, we also compute a polarization observable, called photon asymmetry, defined by

$$\Sigma = \frac{d^3\sigma_{\perp} - d^3\sigma_{\parallel}}{d^3\sigma_{\perp} + d^3\sigma_{\parallel}} \quad (7)$$

where \perp and \parallel denote the perpendicular and parallel photon polarizations relative to the production plane (x-z plane). We have used the short-hand notation $d^3\sigma \equiv d^3\sigma/dE_{\pi}d\Omega_{\pi}d\Omega_N$ with appropriate sums over spin labels implied. Note that the measurement of Σ requires linearly polarized photon beams.

The dependence of the reaction on the nuclear structure is minimal. It enters through the spectroscopic factor S_{α} and the single particle bound wavefunction. The former is an overall normalization factor whose value can be taken from electron scattering. It cancels out in the photon asymmetry. The latter can be sufficiently described by harmonic oscillator wavefunctions in the quasifree region we are interested in.

The final state interaction of the outgoing nucleon with the residual nucleus is described by optical potentials. We use the global optical model by Cooper *et al* [19] based on Dirac phenomenology that successfully describes the nucleon scattering data over a wide range of nuclei ($12 \leq A \leq 208$) and energies (up to around $T_N = 1000$ MeV). To generate the distorted wavefunctions for our formalism, we numerically solved the Schrödinger equation using the Schrödinger equivalent potentials of the model.

For the outgoing pion distorted waves, we numerically solved the Klein-Gordon equation with the first-order optical potential by Gmitro *et al* [20]. It is a microscopic global potential

based on multiple scattering theory and supplemented by πN phase shifts. It gives an excellent description of the pion scattering data for nuclei $4 \leq A \leq 40$ up to around $T_\pi = 400$ MeV and valid up to $T_\pi = 1000$ MeV. We have checked that at low energies ($T_\pi \leq 220$ MeV), it is consistent with the phenomenological SMC pion optical potential [21] which was the traditional choice for low energy pions.

For the kinematics we will consider in the reaction, the kinetic energies of the pion and the nucleon vary in a wide range, up to about 900 MeV. Both are well covered by the optical potentials considered. The integral in Eq. (6) was evaluated numerically using techniques established in our earlier work [15]. To reach convergence, 10 to 15 partial waves were needed for the pion and around 20 partial waves for the nucleon.

All the dynamics of the photoproduction process is contained in the elementary operator $t_{\gamma\pi}$ in Eq. (6), which was usually given in terms of CGLN amplitudes. To use it in a nuclear calculation, we extrapolated the amplitudes off-shell to account for the Fermi motion of the bound nucleon, and performed necessary transformations into appropriate reference frames. For our values of the momentum transfer, the effects of the off-shell extrapolation were found to be quite small.

III. RESULTS

A. The elementary process

Recently the model of Ref. [8] was improved substantially by including more resonances and the new data from Mainz [11]. The new model includes the spin-1/2 resonances $P_{11}(1440)$ (the Roper resonance), $S_{11}(1535)$, $S_{11}(1650)$, the spin-3/2 resonances $P_{33}(1232)$, $D_{13}(1520)$, $D_{33}(1740)$, and the spin-5/2 resonance $F_{15}(1680)$. The resonances are described by Breit-Wigner parameterizations which have been unitarized by including energy-dependent phases that have been adjusted to reproduce the appropriate multipole data. The Born terms include the standard contributions from the nucleon, and the vector

mesons ρ and ω . This model is intended for photon energies up to about 1.1 GeV. Among the considered resonances, the D_{13} is the dominant one in the second resonance region (around $E_\gamma=750$ MeV), while the F_{15} is the dominant one in the third resonance region (around $E_\gamma=1000$ MeV).

To get an idea on the overall quality of the elementary operator, we first compare its predictions for the total cross section with available data in Fig. 1. Also shown are predictions for the photon asymmetry. The three theoretical curves correspond to the full results (solid lines), the results with the D_{13} resonance turned off (dotted lines), and with the F_{15} resonance turned off (dashed lines). Overall, the model gives a good description of the data. The cross section results clearly show a second peak beyond the delta region, more so in the charged pion channels than in the neutral pion channels, which is dominated by the D_{13} resonance. A third peak is most apparent in the π^+n channel, due to the F_{15} resonance. It is interesting to observe that the photon asymmetry displays much larger sensitivities to the D_{13} and F_{15} resonances than the cross sections, especially to the D_{13} resonance in the neutral pion channels. Measurements of this polarization observable in the higher energy region will undoubtedly put more stringent tests on the basic ingredients in the elementary process.

B. Quasifree kinematics

Now we turn to nuclear calculations for the reaction $A(\gamma, \pi N)A - 1$. As noted above, there is a great deal of kinematic flexibility in this reaction. Here we decide to present our calculations under quasifree kinematics. It is achieved by solving Eq. (2) and Eq. (3) at fixed E_γ and $|\mathbf{p}_m|$ and θ_π . The quasifree kinematics closely resembles the two-body kinematics in free space, except here it is on a bound nucleon with momentum p_m . The energies are very close to those in free space (with small influences from nuclear binding and recoil). The nucleon angle will be shifted from its free space value by a certain amount depending on the value of p_m . This kinematic arrangement has the feature that the variables vary in a wide range, maximally exposing the underlying dynamics in the elementary operator, while

TABLE I. Quasifree kinematics for the reaction $^{12}\text{C}(\gamma, \pi^- p)^{11}\text{C}_{g.s.}$ at $E_\gamma = 750$ MeV in the laboratory frame. The numbers in parentheses are the corresponding solutions on the free nucleon.

θ_π (deg)	T_π (MeV)	T_p (MeV)	θ_p (deg)
30	520.8 (538.2)	72.2 (72.3)	74.7 (72.3)
60	382.9 (398.4)	210.1 (212.0)	49.9 (42.4)
90	269.9 (283.0)	323.1 (327.4)	34.0 (27.9)
120	200.3 (211.5)	392.7 (399.0)	22.6 (16.9)
150	164.8 (174.7)	428.2 (435.7)	13.6 (8.0)

being minimally sensitive to the details of the nuclear wavefunction. It benefits studies of the final state interactions as well as the elementary process.

We will limit ourselves to coplanar set-ups with the nucleon on the opposite side of the pion ($\phi_N = 180^\circ$). Such set-ups generally result in larger cross sections than out-of-plane set-ups. We will use ^{12}C as an example. Other nuclei could be studied straightforwardly. Specifically, we will present results for the reaction $^{12}\text{C}(\gamma, \pi N)X_{g.s.}$ (the final nucleus X is either ^{11}C or ^{11}B left in its ground state) with $p_m=100$ MeV/c. This value of p_m yields large counting rates for p-shell nuclei since a 1p-shell nucleon wavefunction has its maximum value at roughly that value. As an example, we give in Table I the numerical solutions for the kinematics at $E_\gamma = 750$ MeV for this reaction in the $\pi^- p$ channel. Small differences occur in the other three channels due to small mass differences of the particles. Both the pion and the nucleon are more energetic in the forward directions. The nucleon tends to stay in the forward direction due to its heavier mass. These numbers also demonstrate the influence of the nuclear binding effects as discussed above.

An important aspect of the reaction is the final state interaction (FSI) of the exiting pion and nucleon with the residual nucleus. They are accounted for by optical models taken from elastic scattering. Here the reaction also serves as a testing ground of these models in a wide energy range. Fig. 2 shows the effects of final state interactions in the $\pi^- p$ channel. To ensure wide kinematical coverage, the total and individual FSI effects on the coincidence

cross section ($d^3\sigma$) and the photon asymmetry (Σ) are shown in two distributions: as a function of E_γ at two fixed values of θ_π , and as a function of θ_π at two fixed values of E_γ .

First we examine the cross sections. The effects of the nucleon FSI alone are relatively small, causing almost an overall reduction of less than 20%. The effects of the pion FSI alone are more significant. In the energy distributions at $\theta_\pi = 60^\circ$, they are large (about a factor of 2) below $E_\gamma=800$ MeV, and become quite small after that. This behavior is consistent with the fact from elastic scattering that pion distortion decreases with increasing energy. The T_π in this case grows from about 40 MeV to 400 MeV as E_γ increases from 300 MeV to 1100 MeV. At $\theta_\pi = 120^\circ$, T_π changes from about 80 MeV to 690 MeV. In the angular distributions, pion distortion is more significant at backward angles (up to a factor of 2 reduction) than at forward angles (almost no reduction), and results in a non-smooth angular distribution. We have checked that the results are convergent by varying the number of partial waves and integration points. To further check this behavior, we repeated the same calculation by setting the elementary operator to unity and found that the resulting distribution was rather smooth. This suggests that the non-smooth behavior was due to the interference between the pion FSI and the elementary process. As a result, the total distortion largely follows the shapes of the pion distortion with additional reduction due to the nucleon distortion.

As for the photon asymmetry, the inclusion of FSI results in almost no changes in this observable in all instances. This situation is similar to our previous findings in quasifree pion and eta photoproduction [15,17,16]. Furthermore, the photon asymmetry is not sensitive to the nuclear structure input as alluded to earlier. We have examined FSI effects in the other three channels, and found similar effects which will not be shown here.

The insensitivity of the photon asymmetry to FSI and to nuclear structure opens the way to use this observable to study possible modifications of the basic production process in the nuclear medium. Such modifications may manifest themselves through variations in the parameters of the resonance such as the mass, the width and the coupling constant (strength). It is expected that its mass would be decreased from interactions via a nuclear potential. Additional channels might open in the medium, causing an increase in its decay

width. The coupling at the interaction vertices might also be modified. To perform a phenomenological sensitivity study of the D_{13} and F_{15} resonances, we apply a 3% decrease in their masses and a 60% broadening of their widths in the elementary operator. These values are in line with those suggested by an cooperative damping model of the resonances [22]. As for the strength, we use the values suggested by a quark exchange model [23]: a reduction of the D_{13} strength by 12% and the F_{15} strength by 22%. We do not claim any validity of these models, but are mostly interested in exploring sensitivity of the observables to possible changes in the resonance parameters. Rigorous studies of such effects clearly require a more dynamical treatment, as in the delta-hole model.

In Figs. 3 to 6, we present the possible medium effects at kinematics similar to Fig. 2. The energy distribution for the D_{13} is shown at a forward angle of $\theta_\pi = 60^\circ$, while for the F_{15} it is shown at $\theta_\pi = 120^\circ$. The angular distributions are shown at E_γ sitting on top of the resonances, at 750 MeV and 1000 MeV. Fig. 3 shows the effects of medium modifications for the process $^{12}\text{C}(\gamma, \pi^- p)^{11}\text{C}_{g.s.}$. The four curves correspond to the full results (solid), the results with the mass decreased by 3% (dotted), with the width increased by 60% (dashed), and with the strength decreased by 12% for D_{13} and 22% for F_{15} (dot-dashed). The results are most sensitive to changes in the resonance mass, followed by the resonance width. The sensitivity to the resonance strength is surprisingly small. In the cross sections, the small reduction of the D_{13} mass results in a large shift of the second peak as well some reduction in the energy distributions, and a large reduction in the angular distributions. The effects of the change in width are also quite large. As for the ‘cleaner’ photon asymmetry, there is a noticeable effect due to the mass change for the D_{13} in the energy distribution, and a very large sensitivity to the F_{15} in the angular distribution. These effects are large enough to be detected by experiments.

Fig. 4 shows the same effects in the π^+n channel. Here all changes in the F_{15} act to damp out the third peak in the energy distribution. Similar sensitivities to the D_{13} are observed. For completeness, the same distributions are shown in Fig. 5 for the $\pi^0 p$ channel, and in Fig. 6 for the $\pi^0 n$ channel. It should be pointed out that these calculations were done in

DWIA, so the effects in the cross section are *relative* effects on top of the FSI effects. The effects in the photon asymmetry are almost purely signatures of medium modifications, as discussed earlier.

IV. CONCLUSION

Using a tree-level model for single pion photoproduction on the nucleon at higher energies, we have performed calculations for the exclusive photonuclear reaction, $A(\gamma, \pi N)A - 1$, in the distorted wave impulse approximation, for photon energies up to about 1.1 GeV. The reaction has the kinematical feature that it allows small momentum transfers. In the quasifree region (< 400 MeV/c), the reaction is not sensitive to the nuclear structure input, and provides one of the cleanest ways to study nucleon resonances in the nuclear medium.

Final state interactions are incorporated via optical potentials and are found to substantially reduce the cross sections, especially at backward pion angles, but not affect the photon asymmetry.

To shed light on the ‘damped resonances’ in the second and third resonance regions as seen in total nuclear photoabsorption data, we explored the effects of possible medium modifications of the D_{13} and F_{15} resonances by varying their parameters using model guidance. It is found that this reaction is very sensitive to such changes in these resonances. Especially if the photon asymmetry is measured, the effects can easily be detected by experiments. We therefore believe that measurements of exclusive quasifree pion photoproduction with polarized photons are an important future step that should help untangle the riddle of the damped resonances.

ACKNOWLEDGMENTS

This work was supported in part by U.S. DOE under Grants DE-FG03-93DR-40774 (F.L.), DE-FG02-95ER-40907 (C.B.), and DE-FG02-87ER-40370 (L.W.).

REFERENCES

- [1] K.I. Blomqvist and J.M. Laget, Nucl. Phys. **A280**, 405 (1977); J.M. Laget, Nucl. Phys. **A481**, 765 (1987).
- [2] R.M. Davidson, N.C. Mukhopadhyay, and R.S. Wittman, Phys. Rev. D **43**, 71 (1991).
- [3] S. Nozawa, B. Blankleider, and T.-S. H. Lee, Nucl. Phys. **A513**, 495 (1990); S. Nozawa, T.-S. H. Lee, and B. Blankleider, Phys. Rev. C **41**, 213 (1990).
- [4] H. Sato and T.-S. H. Lee, Phys. Rev. C **54**, 2660 (1996).
- [5] Y. Surya and F. Gross, Phys. Rev. C **53**, 2422 (1996).
- [6] K. Nakayama *et al.*, *Proceedings of the 4th CEBAF/INT Workshop on N* Physics*, INT, Seattle, Sept.9-13, 1996 (World Scientific, Singapore, 1997, T.-S. H. Lee and W. Roberts, editors), p. 156.
- [7] T. Feuster and U. Mosel, nucl-th/9803057.
- [8] O. Hanstein, Diploma thesis, University of Mainz, 1993 (unpublished).
- [9] H. Garcilazo, E. Moya de Guerra, Nucl. Phys. **A562**, 521 (1993).
- [10] M. Guidal, J.M. Laget, M. Vanderhaeghen, Nucl. Phys. **A627**, 645 (1997).
- [11] S.S. Kamalov, D. Drechsel, O. Hanstein, and L. Tiator, Mainz preprint, to be published.
- [12] VPI Group. The data can be viewed and retrieved via the SAID program at the website:
<http://clsaid.phys.vt.edu/~CAPS/>.
- [13] K. Ukai and T. Nakamura (INS, University of Tokyo), Report No. INS-T-550 (1997).
Part of the data can be viewed at http://www.tanashi.kek.jp/~ukai/index_e.html.
- [14] N. Bianchi *et al.*, Phys. Lett. **B229**, 219 (1993), Phys. Lett. **B309**, 5 (1993), Phys. Lett. **B325**, 333 (1993), Phys. Rev. C **54**, 1688 (1996); M. Anghinolfi *et al.*, Phys. Rev. C **47**, R992 (1993). M. MacCormick *et al.*, Phys. Rev. C **55**, 1037 (1997).

- [15] F.X. Lee, L.E. Wright, C. Bennhold, Phys. Rev. C **48**, 816 (1993).
- [16] F.X. Lee, C. Bennhold, L.E. Wright, Phys. Rev. C **55**, 318 (1997).
- [17] F.X. Lee, L.E. Wright, C. Bennhold, and L. Tiator, Nucl. Phys. **A603**, 345 (1996).
- [18] F.X. Lee, C. Bennhold, L.E. Wright, T. Mart, in preparation.
- [19] E.D. Cooper, S. Hama, B.C. Clark, and R.L. Mercer, Phys. Rev. C **47**, 297 (1993).
- [20] M. Gmitro, S.S. Kamalov, and R. Mach, Phys. Rev. C **36**, 1105 (1987).
- [21] K. Stricker, H. McManus, and J.A. Carr, Phys. Rev. C **19**, 929 (1979); **22**, 2043 (1980); **25**, 952 (1982).
- [22] M. Hirata, K. Ochi, and T. Takaki, nucl-th/9711017.
- [23] M.M. Giannini and E. Santopinto, Phys. Rev. C **49**, R1258 (1994).

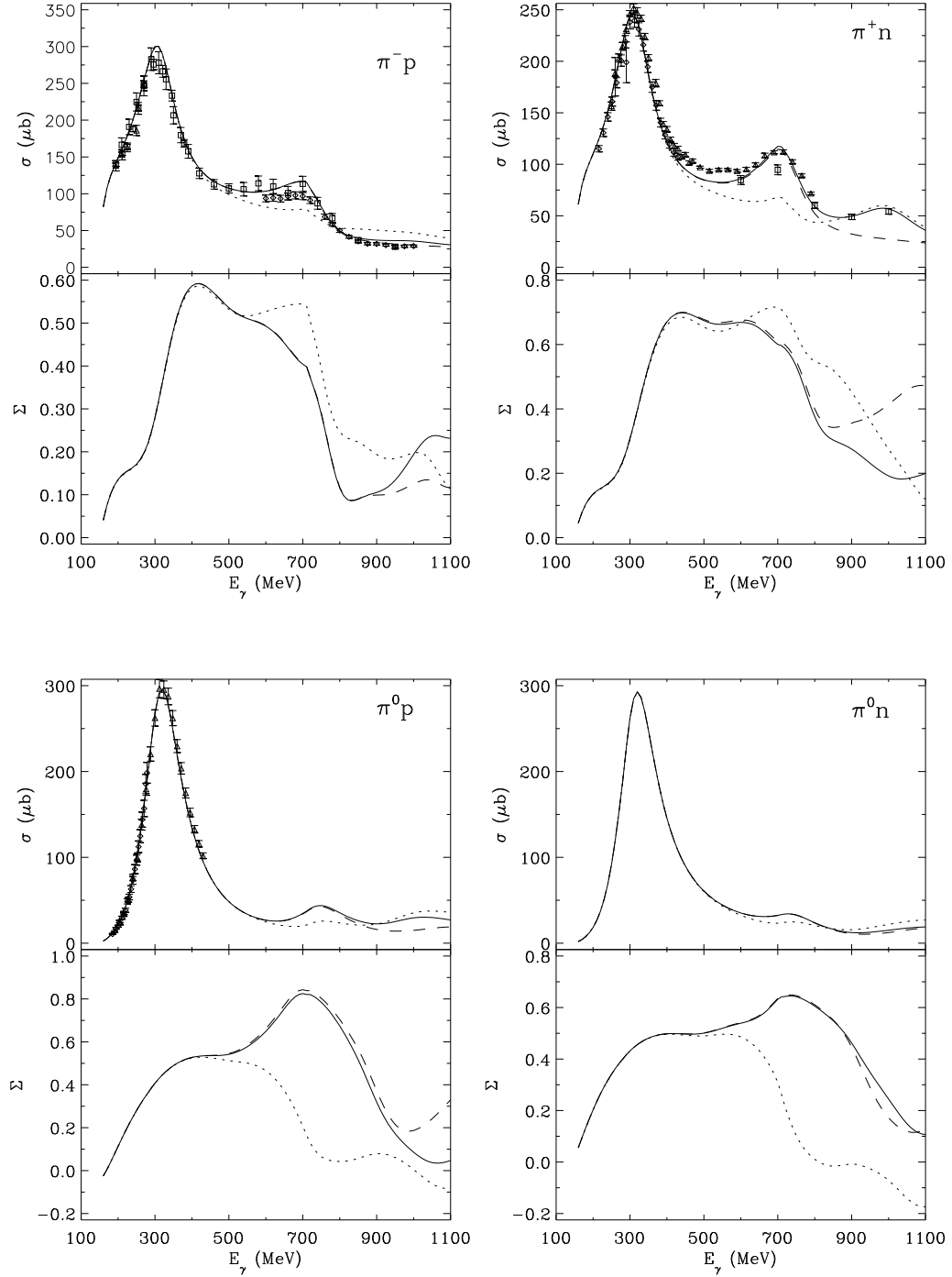


FIG. 1. Total cross section and photon asymmetry for the free process in the four channels. The three curves correspond to results with the full operator (solid), with D_{13} turned off (dotted), and with F_{15} turned off (dashed). The data points are from [12] and [13].

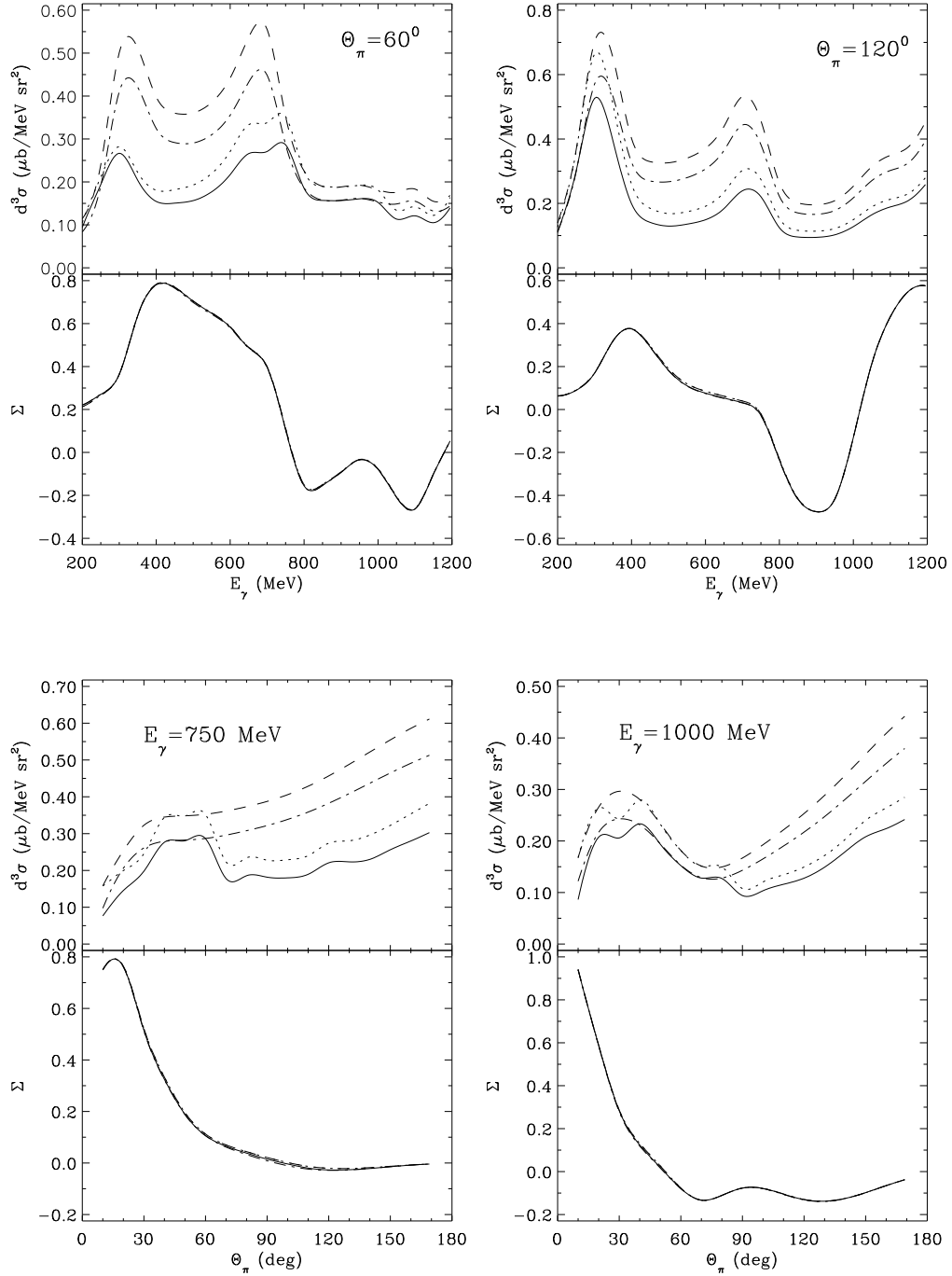


FIG. 2. Effects of final state interactions in the reaction $^{12}\text{C}(\gamma, \pi^- p)^{11}\text{C}_{g.s.}$. The upper two panels are photon energy distributions at fixed pion laboratory angles, while the lower two are pion angular distributions at fixed photon energies. The four curves correspond to calculations in PWIA (dashed), in DWIA with pion distortion only (dotted), with nucleon distortion only (dash-dotted), and with both distortions (solid).

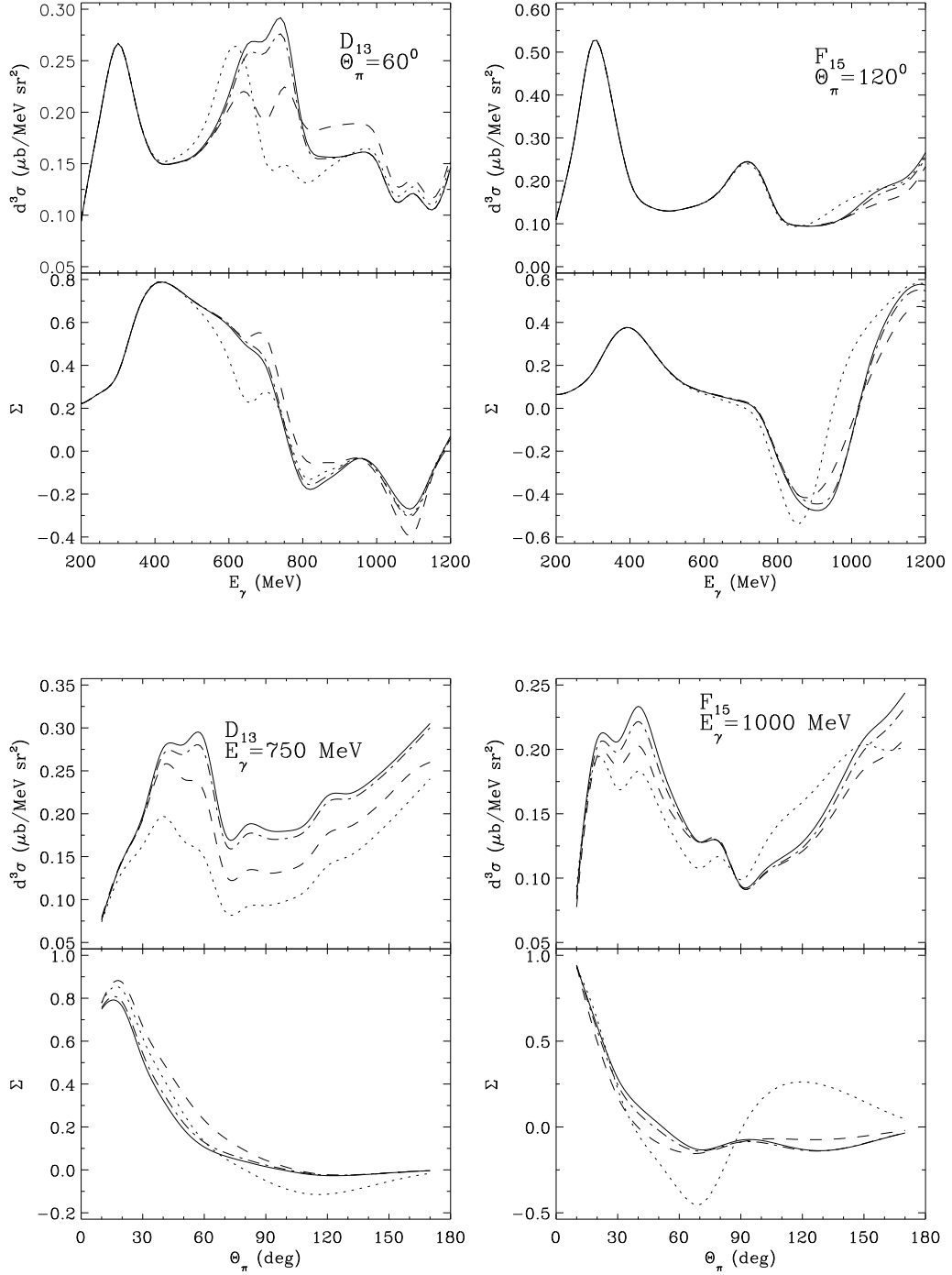


FIG. 3. Effects of possible medium modification of the $D_{13}(1520)$ and $F_{15}(1680)$ resonances in the reaction $^{12}\text{C}(\gamma, \pi^- p)^{11}\text{C}_{g.s.}$. The four curves correspond to the full results (solid), with the mass decreased by 3% (dotted), with the width increased by 60% (dashed), and with the strength decreased by 12% for D_{13} and 22% for F_{15} (dot-dashed). The calculations were done in DWIA.

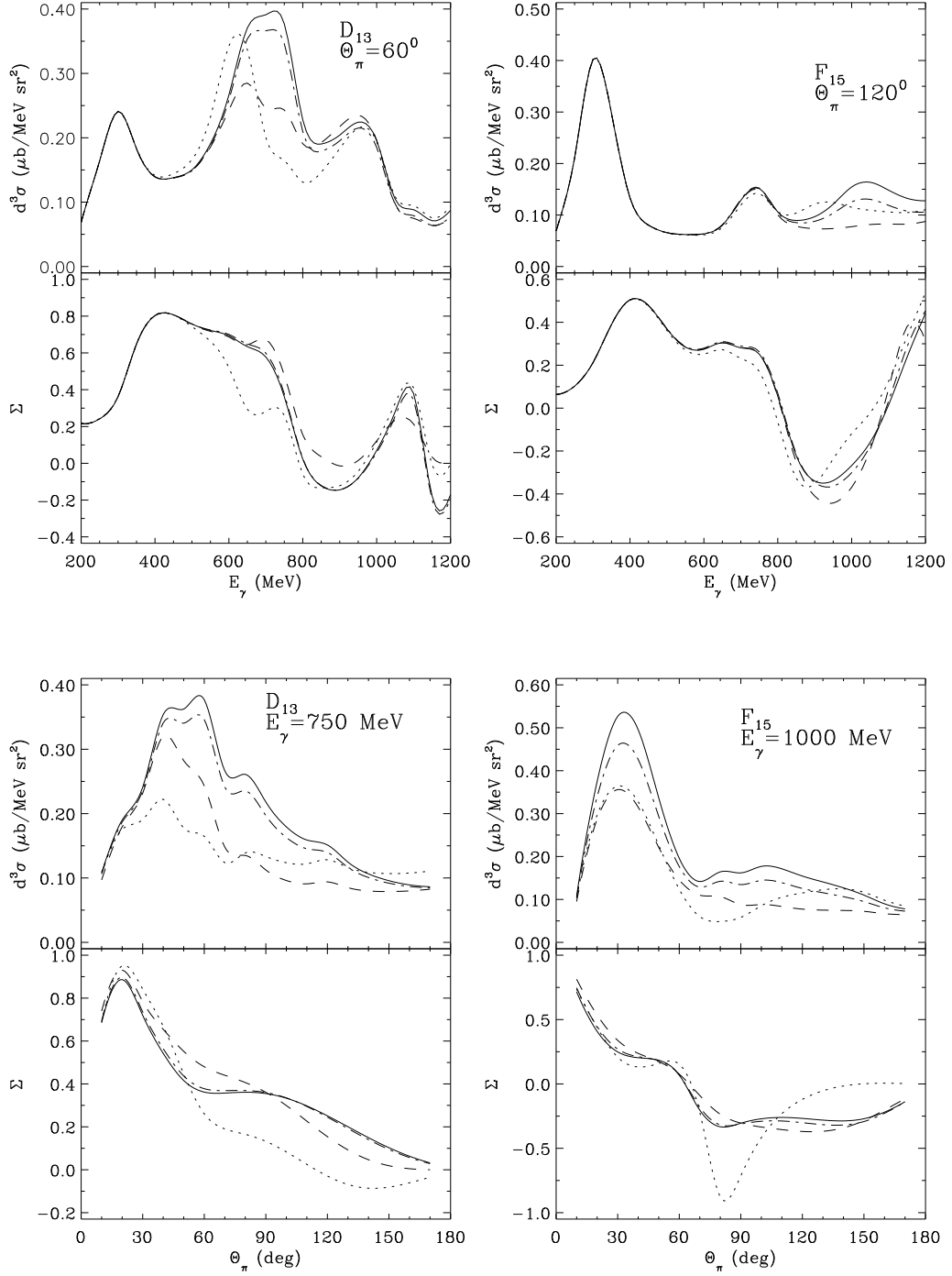


FIG. 4. Similar to Fig. 3, but for the π^+n channel.

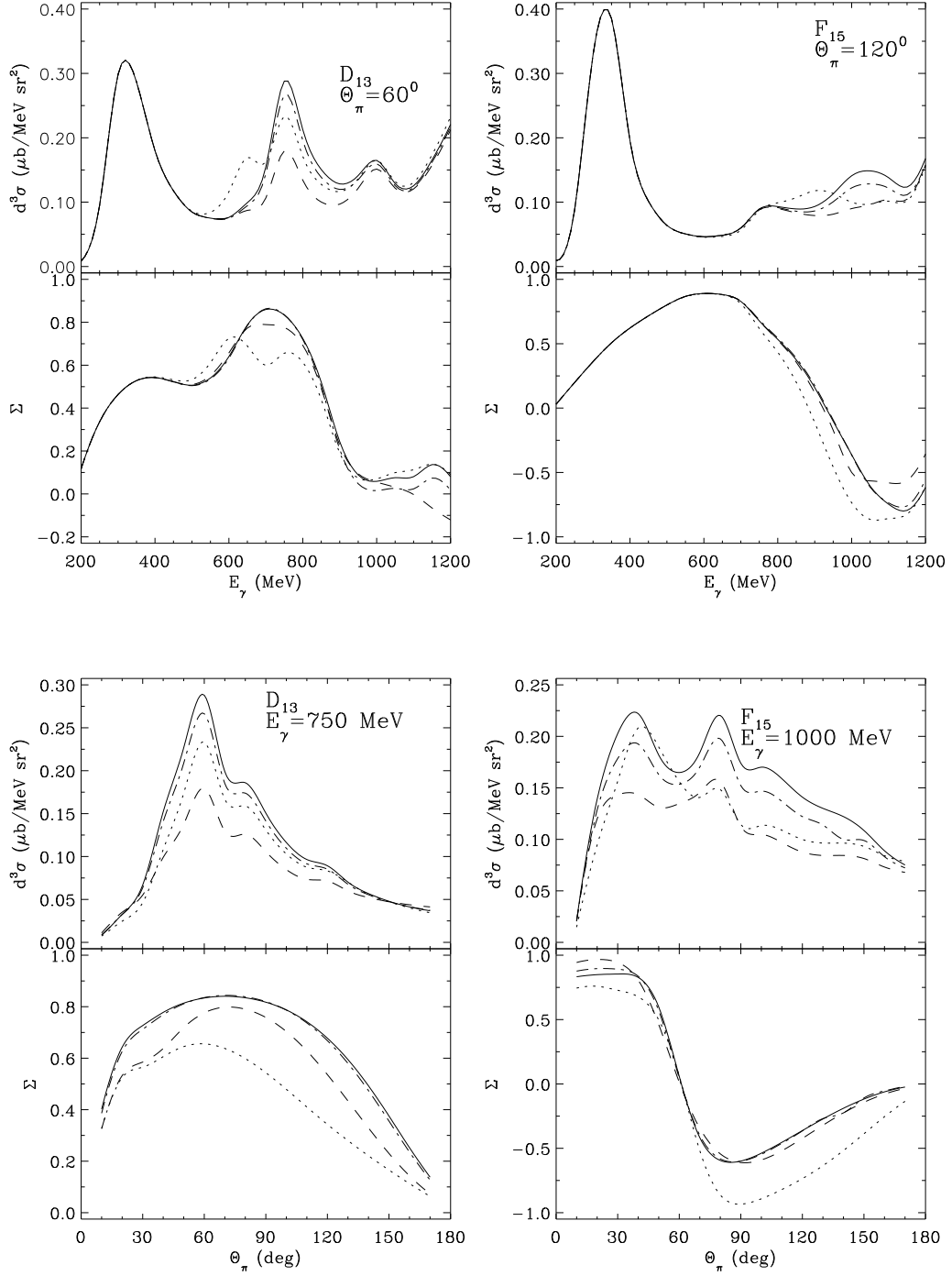


FIG. 5. Similar to Fig. 3, but for the $\pi^0 p$ channel.

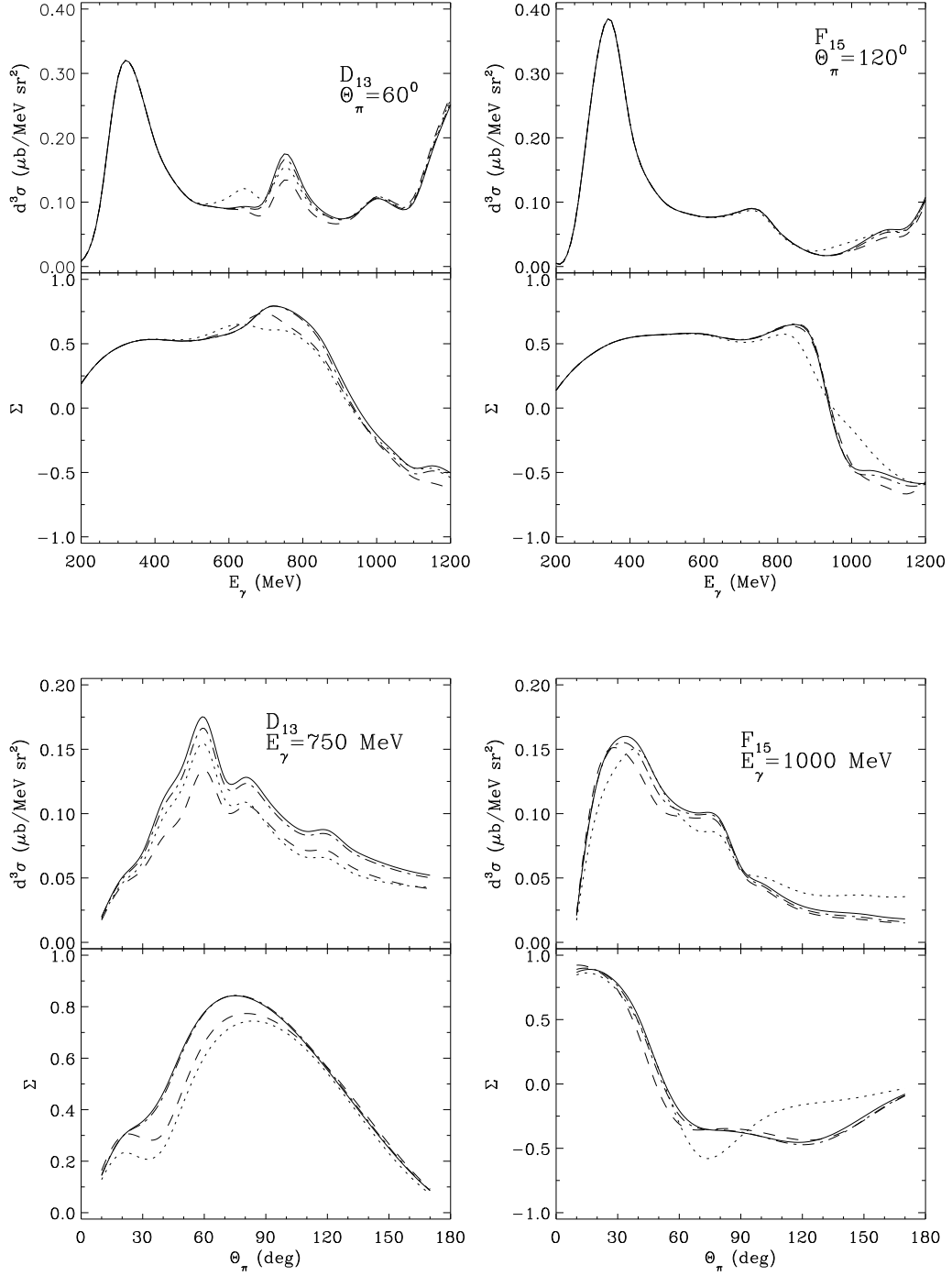


FIG. 6. Similar to Fig. 3, but for the $\pi^0 n$ channel.